2. V. I. Marusev et al., "Comprehensive apparatus for recording and processing of experimental data in materials research by the electrical resistance method," Preprint NIIAR 39 (604) [in Russian], Scientific-Research Institute of Atomic Reactors, Dimitrovgrad (1983), 8 pp.
3. Kh. Ya. Bondars and A. A. Lapenas, Izv. Akad. Nauk Latv. SSR, Ser. Fiz. Tekh. Nauk, No. 2, 3 (1980).

STUDY OF MASS TRANSFER OF IMPURITIES IN SODIUM

F. A. Kozlov and V. A. Likharev

UDC 621.039.534.63

Hydrogen and oxygen are the main impurities that enter into the sodium coolant during the operation of reactor plants. Experiments with plugging meters and models of traps have yielded contradictory results on the mechanism of the mass transfer, the conditions of the existence of a crystal phase of these impurities, and the role of this phase in the formation of a layer of deposits in cold traps. Studies on models of traps involving cutting and analysis of the accumulated impurity are laborious.

The proposed procedure for studying the mass transfer of the impurities (products of the interaction of sodium with water) is based on the determination of the thermal resistance of the layer of impurities deposited from a nonisothermal sodium flow onto a stationary mass-transfer surface. The resistance was calculated from the depth to which traveling thermocouples were embedded in the wall of the cooled tube of the clean segment (Fig. 1) in seven cross sections along the length of the heat-exchange zone. The embedding depth was determined on the basis of a calculation for the clean segment, measuring the temperature along the length of the jacket of the heat exchanger, the walls of the central tube, and on the axis of the sodium flow. For this purpose the thermal flux in the segment of thermal stabilization of the NaK alloy and the coolant velocity (Na and NaK alloy) over the cross section of the channels were assumed to be constant while the radial distribution of the temperature was assumed to be a third-degree polynomial. Extrapolation was used in the segment of thermal stabilization of the sodium. The effect of axial heat leaks, which manifested itself at a sodium Péclet number of less than 100, was taken into account with a correction, whose value was assumed to be proportional to the gradient of the mean mixed

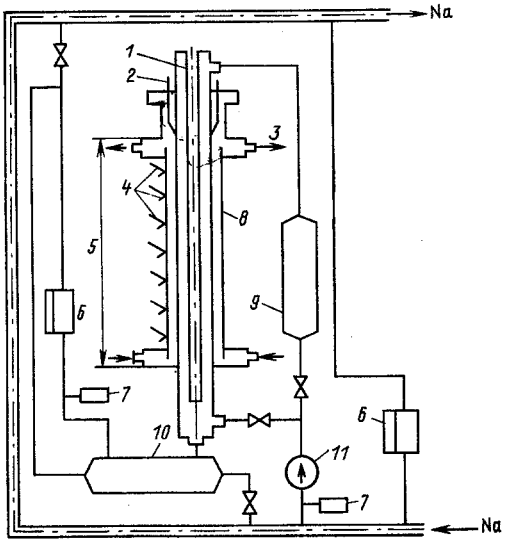

Fig. 1. Experimental section and the diagram of its location in the sodium loop: 1) thermocouple jacket; 2) traveling thermocouple; 3) NaK alloy; 4) thermocouples; 5) heat-exchange zone (700 mm); 6) IVA hydrogen sensor; 7) oxygen cell; 8) experimental segment; 9) heat exchanger; 10) recuperator; 11) pump.

Translated from Atomnaya Énergiya, Vol. 65, No. 1, pp. 62-64, July, 1988. Original article submitted May 14, 1987.

 0038-531X/88/6501-0614$12.50

TABLE 1. Experimental Regimes and Crystallization (dissolution) Parameters

Regime	Flow rate, kg/sec	Re	Sodium temp., K		Concn. of O(H) at inlet, ppm	Impurity accumulation, g	Density of layer, vol.%	Mass-transfer coeff., $KF \cdot 10^4$	Duration of expt., 10^{-3} sec
			inlet	outlet					
1	0,350	19100	559	475	52,1	69,0 (Na_2O)	6,1	1,111	8,39
2	0,247	13400	554	485	46,2	25,2 (Na_2O)	7,6	0,292	13,50
3	0,178	8500	523	442	31,0	44,9 (Na_2O)	9,4	0,528	12,60
4	0,151	9100	540	537		27,6 (NaH)	17,1	1,111	7,24
5	0,151	9100	541	538		21,6 (NaH)	4,9	1,472	6,01
6	0,375	20400	543	499	4,0	20,2 (NaH)	35,1	3,69 ($N=1$) 0,131 ($N=2$)	25,4
7	0,261	13600	543	471	3,5	34,6 (NaH)	25,4	7,69 ($N=1$) 0,192 ($N=2$)	11,4
8	0,153	7200	541	435	3,8	36,9 (NaH)	4,5	5,42 ($N=1$) 0,117 ($N=2$)	13,25

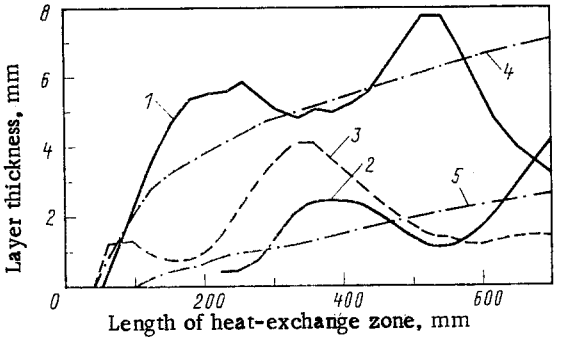

Fig. 2. Distribution of the layer of sodium oxide deposits during crystallization: 1, 2, 3) from calculation of the thermal resistance of the layer for regimes Nos. 1, 2, and 3, respectively; 4, 5) regimes Nos. 1 and 2, from calculation of the average mass-transfer coefficient.

temperature of the sodium along the length of the flow. The proportionality factor was found from the condition that the sodium temperature decrease upon entering the heat-exchange segment in comparison with the temperature from this segment (measured experimentally). The thermal conductivity coefficient of the impurity layer for the case of sodium oxide was taken from the data of [1]. The computational error in the determination of the impurity layer thickness was ±12%. The length of the segment of thermal stabilization of the NaK alloy was determined from [2].

The amount of accumulated impurity was determined by its transfer from the segment into the sodium loop, measuring the impurity concentration in the loop to within ±15%. The hydrogen concentration in the sodium was measured with plugging meters based on magnetic-discharge pumps while the oxygen concentration was measured with electrochemical cells. Oxygen and hydrogen were introduced into the sodium loop in the gaseous state.

The value of the mass-transfer coefficient for a motionless mass-transfer surface was found from the expression for the impurity balance in the absence of bulk crystallization

$$-V\,dC_L/dx = KF\pi D\,(C_L - C_W)^N,$$

where V is the sodium flow rate (m^3/sec), C_L and C_W are the impurity concentration in the sodium flow and the saturation concentration determined from the solubility curve for oxygen [3] and hydrogen [4] at the temperature of the mass-transfer surface (g/m^3), F is a coefficient that allows for the increase in the mass-transfer surface in comparison with the clean surface, D is the channel diameter (m), and K is the mass-transfer coefficient, m/sec (N = 1) and $m^4/[g(NaH) \cdot C]$ (N = 2).

In Table 1 regimes Nos. 4 and 5 pertain to an experiment on the dissolution of the sodium hydride accumulated in the segment and the other regimes pertain to crystallization experiments. The values of KF in the experiments on crystallization of sodium oxide and

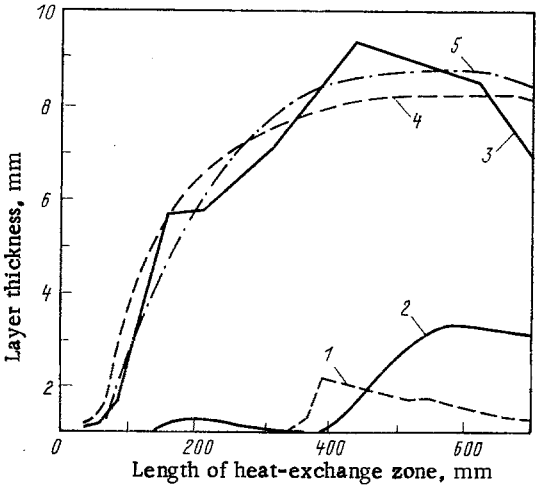

Fig. 3. Distribution of the layer of sodium hydride deposits during crystallization: 1, 2, 3) from calculation of the thermal resistance of the layer for regimes Nos. 6, 7, and 8, respectively; 4, 5) from calculation of the mass-transfer coefficient for regime No. 8 for N = 1 and N = 2, respectively.

dissolution of sodium hydroxide (regimes Nos. 1-5) were calculated on the assumption of a diffusion mechanism of transfer and in experiments on the crystallization of sodium hydride they were calculated for a diffusion mechanism and a limited crystal growth. Using the values of KF, with allowance for the heat-exchange of the segment, we calculated the distribution of the layer of crystallizing impurity over the heat-exchange zone that corresponds to the assumed transfer mechanism. This distribution was compared with that obtained from calculation of the thermal resistance of the impurity layer and on the basis of a comparison we concluded that the assumption concerning the transfer mechanism was correct.

These distributions are observed to correspond approximately (Fig. 2) in the case of crystallization of sodium oxide. The distribution curves obtained from calculation of the thermal resistance display a maximum, which corresponds to an oxygen supersaturation of about 15 ppm in the sodium flow. This indicates that bulk crystallization of sodium oxide is probable. The maximum increase in the mass-transfer surface (regime No. 1) in the experiments was threefold.

In the case of crystallization of sodium hydride, upon comparing the impurity distributions for various transfer mechanisms (Fig. 3), we cannot give preference to one of them. This same conclusion was made by Filder and Saagi [5], who assumed that both mechanisms act at various stages of the process as the result of the variation of the mass-transfer surface. The impurity distributions obtained from calculation of the thermal resistance of the layer (Fig. 3, curves 1 and 2) indicate that the surface plays the determining role in the intensification of the mass transfer. The main result is that when a certain supersaturation is reached the surface of the sodium hydride crystal increases abruptly and the mass transfer, hitherto limited by the crystal growth, will also be determined by hydrogen diffusion toward the surface of the crystal from the sodium flow. This phenomenon was described in [6] and was attributed to the formation of a cellular or dendritic structure of the growing crystal. The corresponding cross section of the heat-exchange zone can be approximated if the temperature of the onset of crystallization at the surface is taken from the saturation curve, which is obtained with the aid of a plugging meter.

In experiments on the dissolution of sodium hydride the value of KF is in agreement with the data of [5, 7] on the crystallization of sodium hydride in a plugging meter ($\sim 9.2 \cdot 10^{-4}$ m/sec). Assuming that F = 1, we find that the hydrogen diffusion coefficient in sodium should be approximately two orders of magnitude higher than the sodium self-diffusion coefficient. This result is at variance with the data of [8] and an unreasonably high value of F (10^3-10^4) must be taken in order to obtain agreement.

From a comparison of the values of KF for crystallization and dissolution it follows that on the whole the crystallization of sodium hydride determined the kinetics of the growth of the surface of crystals in the experiments.

LITERATURE CITED

1. F. A. Kozlov and I. N. Antonov, At. Energ., 19, No. 4, 391 (1967).
2. N. A. Ampleev, P. L. Kirillov, V. I. Subbotin, and M. Ya. Suvorov, "Heat-exchange of liquid metal in a vertical tube at low values of the Pe number," in: Liquid Metals [in Russian], Atomizdat, Moscow (1967), pp. 15-31.
3. J. Noden, J. Brit. Nucl. Energ. Soc., 12, No. 1, 57 (1973).
4. A. Whittingham, J. Nucl. Mater., No. 60, 119 (1976).
5. R. Filder and R. Saagi, J. Brit. Nucl. Energ. Soc., 23, No. 6 (385) (1984).
6. C. Cheng, F. Irvin, and B. Kyle, AIChE J., 13, No. 4, 739-744 (1967).
7. C. Smith et al., J. British Energ. Soc., 18, No. 3, 201 (1979).
8. J. Trouve and G. Laplanche, J. Nucl. Mater., No. 115, 56 (1983).

RADIOACTIVITY INDUCED BY HIGH-ENERGY PROTONS

A. A. Astapov and M. M. Komochkov

UDC 539.125.4.16

Maintenance, tuning, and servicing of proton accelerators imply the irradiation of personnel mainly with the γ radiation of the induced radioactivity which is rather strong. Its contribution to the total personal irradiation dose usually exceeds 60% [1-4].

Data [5] which were obtained with semiempirical approximations [6] of the cross section of radionuclide production in proton-nuclei interactions are one of the principal sources of information for predicting the radiation conditions resulting from the induced radioactivity and for selecting construction materials of lowest activation levels.

The later approximations of [7] describe in greater detail the production cross sections of light nuclear products, e.g., ^{7}Be; the approximations of [6] for the light nuclear products can differ from the experimental values by factors of a few tens. The approximations of [7] can be used to introduce the products of peripheral reactions which under certain conditions significantly contribute to the dose of the induced radioactivity. Besides that, the approximations of [7] for target nuclei with an order number $Z \lesssim 20$ are very precise: the standard deviation of the calculated spallation cross sections from the experimental values does not exceed 30% [7].

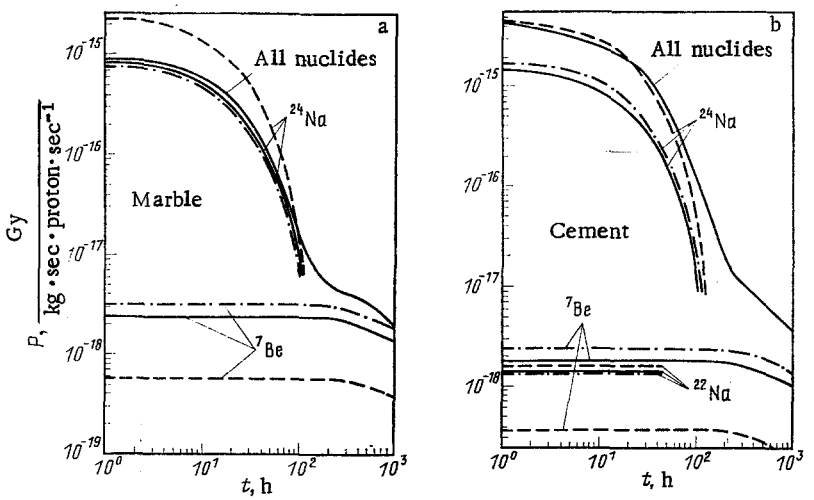

Fig. 1. Time dependencies of the absorbed dose rate P(t) of ^{7}Be, ^{24}Na, and all radionuclides produced in a) marble and b) cement after 1-h irradiation with 12-GeV protons (—— refers to the experiment of [8]; — — — refers to the calculations of [6]; and —·—·—·— refers to the calculations of [7]).

Translated from Atomnaya Énergiya, Vol. 65, No. 1, pp. 64-65, July, 1988. Original article submitted May 26, 1987.

0038-531X/88/6501-0617$12.50